EPJ Web of Conferences **126**, 04004 (2016) DOI: 10.1051/epjconf/201612604004
ICNFP 2015

Top quark pair properties using the ATLAS detector at the LHC

Gaetano Barone[1 a]
On behalf of the ATLAS Collaboration

[1] *Brandeis University*

Abstract. These proceeding review the most recent results on the top quark measurements performed by the ATLAS detector, based upon datasets of 4.59 fb^{-1} and of 20.3 fb^{-1} of proton–proton collisions delivered by the Large Hadron Collider at the centres-of-mass energy of $\sqrt{s}$ = 7 TeV and of $\sqrt{s}$ = 8 TeV, respectively. The measurements of the top quark mass, the cross section of $t\bar{t}$ production in association of vector bosons (W, Z and γ) and the measurement of the charge asymmetry are detailed. The importance of evermore precise measurement of the top quark's properties is highlighted.

1 Introduction

The discovery of the top quark (t) ages, nowadays, twenty years, however, many of its properties are yet to fully constrained by the experiment. The top quark possesses a Yukawa coupling to the Higgs boson of $O(1)$ and a mass close to the scale of the Electro Weak Symmetry Braking (EWSB), on which the modern understanding of particle physics is based. Moreover, because of its large mass, thus decaying before forming bound states, and because of its almost single decay mode trough $t \to Wb$ several of its properties are directly transferred to its decay products. Undiscovered physical phenomena connected with the EWSB can manifest themselves through deviations from the predictions of the Standard Model (SM) in top quark observables. At the Large Hadron Collider (LHC), top quarks are abundantly produced tough Electro Weak (EW) interactions, so called single top, ($pp \to W^\star \to tb$) or in pairs ($t\bar{t}$) via either the strong interaction ($pp \to g \to t\bar{t}$) or EW interaction ($pp \to \gamma^\star(Z^\star) \to t\bar{t}$). Therefore, top related physics at the LHC provide an important framework for a stringent testing of the SM and for the search of new phenomena.

These proceedings focus on the measurements of the top quark properties performed by the ATLAS detector with datasets of proton–proton collisions at the centre-of-mass energies of $\sqrt{s}$ = 7 TeV and 8 TeV delivered by the LHC. The most recent results of the top quark mass (m_{top}) are reviewed in Sec. 2. The measurements of $t\bar{t}$ production in association with vector bosons ($t\bar{t}V$) are discussed in Sec. 3. The review of the top quark properties is concluded by the review on the results of the charge asymmetry in Sec. 4. The concluding remarks are discussed in Sec. 5.

2 Top quark mass

The top quark mass is one of the free parameters of the SM, radiative and loop corrections relate m_{top} to the Higgs boson and to the W–boson. Therefore, the accurate experimental determination of m_{top}

[a] e-mail: gaetano.barone@cern.ch

is of great importance for stringent tests of the SM as well as for the evaluations of the stability of the EW vacuum [1].

The most recent results from the ATLAS experiment [2] determine $m_{\mathrm{top}}$with an accuracy of 1 GeV by combining the measurements in the single lepton (ℓ= electron or muon) plus jets final state and di-lepton final state. Both measurements are performed by a kinematic reconstruction of the invariant mass of the top quark decay products which allows for the extraction of the reconstructed top mass (labelled hereafter $m_{\mathrm{top}}^{\mathrm{reco}}$ for the single lepton channel and $m_{\ell b}^{\mathrm{reco}}$ for the di-lepton channel).

A parametrisation of the reconstructed top quark mass in simulation allows for a calibration of the detector response with respect to the value of m_{top} predicted in simulation. In the single lepton decay final state the response is broken down by the leading components of the systematic uncertainty which are the *b*-jet energy scale dependence (BJSF) and the jet energy scale dependence (JSF).

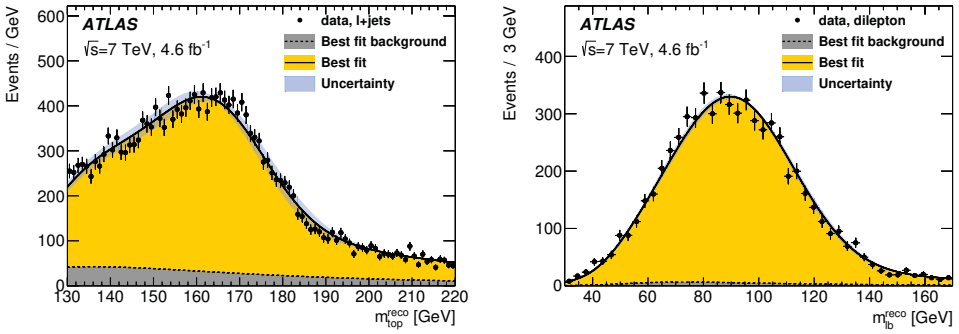

Figure 1. The fitted distributions in the data, showing $m_{\mathrm{top}}^{\mathrm{reco}}$ (left) for the single lepton (electron or muon) final state and $m_{\ell b}^{\mathrm{reco}}$ (right) for the di-lepton final state. The fitted probability density functions for the background alone and for signal-plus-background are also shown. The uncertainty bands indicate the total uncertainty on the signal-plus-background fit [2].

A template fit on data of the parametrised distributions as a function of m_{top}, see Fig. 1, allows for the extraction of the measured top quark mass. The result in the single lepton final state is

$$m_{\mathrm{top}}^{\ell+\mathrm{jets}} = 172.33 \pm 0.75\ (\mathrm{stat.+JSF+bJSF}) \pm 1.02\ (\mathrm{syst.})\ \mathrm{GeV} \tag{1}$$

where the leading systematic uncertainties are due to a residual jet energy scale and jet energy resolution mis-modelling. Respectively, in the di-lepton final state the result is:

$$m_{\mathrm{top}}^{\mathrm{dil}} = 173.79 \pm 0.54\ (\mathrm{stat.}) \pm 1.30\ (\mathrm{syst.})\ \mathrm{GeV} \tag{2}$$

with the leading systematic uncertainty arising from the *b*-jet energy scale mis-modelling. The combination of those two results ($m_{\mathrm{top}}^{\mathrm{comb}}$) corresponds to

$$m_{\mathrm{top}}^{\mathrm{comb}} = 172.99 \pm 0.48\ (\mathrm{stat.}) \pm 0.78\ (\mathrm{syst.})\ \mathrm{GeV} \tag{3}$$

The result of Eq. 3 is among the most precise measurements of the top quark mass to date. However, the definition of the top mass depends upon the renormalisation scheme used in simulation and it lacks a clear interpretation in a well defined theoretical picture. Several theoretical calculations in perturbative quantum chromodynamics identify the top quark mass with the pole mass $m_{\mathrm{top}}^{\mathrm{pole}}$. The pole

mass can be determined experimentally from the inclusive cross section of $t\bar{t}$ pairs ($\sigma_{t\bar{t}}$). Due to the reduced sensitivity of $\sigma_{t\bar{t}}$ to m_{top} and to large uncertainties on the renormalisation and factorisation scales, the measured $m_{\mathrm{top}}^{\mathrm{pole}}$ is of a smaller precision compared to that of the measurement of Eq. 3. However, a novel technique [3] suggests that the measurement of the normalised differential cross section $\mathcal{R}(m_{\mathrm{top}}^{\mathrm{pole}}, \rho_s) = \frac{1}{\sigma_{t\bar{t}+1\mathrm{jet}}} \cdot \frac{d\sigma_{t\bar{t}+1\mathrm{jet}}}{d\rho_s}(m_{\mathrm{top}}^{\mathrm{pole}}, \rho_s)$ for $t\bar{t}$ production with at least one additional jet as a function of the invariant mass of the $t\bar{t}$+1 jet system $\rho_s = \frac{2m_0}{\sqrt{s_{t\bar{t}+1\mathrm{jet}}}}$, with m_0 an arbitrary constant, enhances the sensitivity to the top quark exploiting the phase-space dependence upon the amount of gluon radiation. The measurement of $\mathcal{R}(m_{\mathrm{top}}^{\mathrm{pole}}, \rho_s)$ in a fiducial phase-space within the detector acceptance allows for a reduction upon the theoretical uncertainties entering in the extrapolation from the measured phase-space to the one defined in simulation.

The combination of the these to factors are exploited by the ATLAS experiment and $m_{\mathrm{top}}^{\mathrm{pole}}$ is extracted from a parametrisation on the measured value of $\mathcal{R}(m_{\mathrm{top}}^{\mathrm{pole}}, \rho_s)$, see Fig. 2.

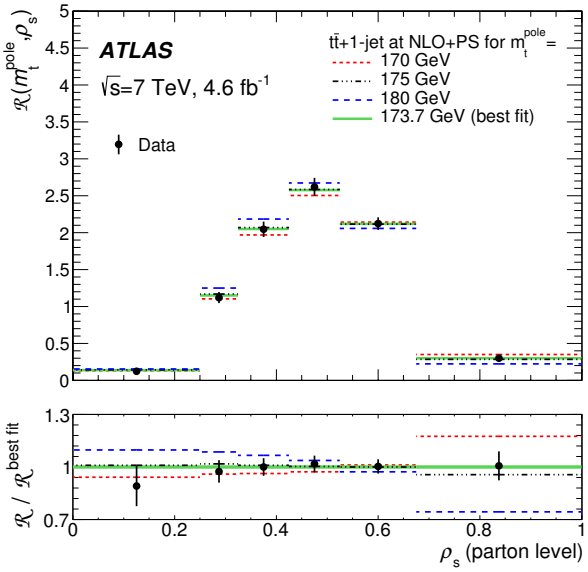

Figure 2. $\mathcal{R}(m_{\mathrm{top}}^{\mathrm{pole}}, \rho_s)$-distribution at parton level corrected for detector and hadronization effects after the background subtraction as a function of $\rho_s(m_0 = 170\ \mathrm{GeV})$. The predictions of the $\sigma_{t\bar{t}+1\mathrm{jet}}$ calculation are performed at next to leading order using three different masses ($m_{\mathrm{top}}^{\mathrm{pole}} = 170, 175$ and 180 GeV) are shown together with the result of the best fit to the data, $m_{\mathrm{top}}^{\mathrm{pole}} = 173.7 \pm 1.5$ (stat.) GeV. The black points correspond to the data. In the lower part of the figure, the ratios of the different R-distributions to the one corresponding to the best fit are shown. The shaded area indicates the statistical uncertainty [1].

The extracted value of $m_{\mathrm{top}}^{\mathrm{pole}}$ [1] corresponds to

$$m_{\mathrm{top}}^{\mathrm{pole}} = 173.7 \ \pm \ 1.5\ (\mathrm{stat.}) \ \pm 1.4\ (\mathrm{syst.})\ ^{+1.0}_{-0.5}\ (\mathrm{theory})\ \mathrm{GeV}, \tag{4}$$

with the measurement being limited by the statistical uncertainty and missing higher order theoretical calculations. The main systematic uncertainties arise from the jet energy scale dependence (0.9 GeV).

3 $t\bar{t}$ plus vector boson

Hypothesised new phenomena, at a higher scale of that accessible by the experiment, can be modelled by effective theories. These models are based upon anomalous couplings of vector bosons ($V = W, Z$ and photon) to the top quark that can be probed through precision measurements at lower scales. For example, models of composite top quarks [4], or with excited top quark production, followed by the radiative decay $t^\star \rightarrow t\gamma$. The measurements of the $t\bar{t}V$ cross sections as performed by the ATLAS collaboration are discussed in the following two sections. Section 3.1 focuses on the $t\bar{t}$ plus photon ($t\bar{t}\gamma$) production cross section, while Sec. 3.2 focuses on the simultaneous measurement of the $t\bar{t}$ plus W ($t\bar{t}W$) and $t\bar{t}$ plus Z ($t\bar{t}Z$) production cross sections.

3.1 Cross section of $t\bar{t}$ production association with a photon

The $t\bar{t}\gamma$ fiducial cross section ($\sigma^{\text{fid.}}_{t\bar{t}\gamma}$) is measured in the single lepton channel characterised by a high-p_{T} electron or muon, at least four high-p_{T} jets, large transverse missing momentum and an energetic photon. The final states of $t\bar{t}\gamma$ production are indistinguishable from the production of background processes which may also feature a final state energetic photon. The contribution of the background processes is estimated using techniques based on data and on well known phenomena, reducing the simulation-induced model-dependency of the result. The response for hadrons, or hadron decay products ($\pi^0 \rightarrow \gamma\gamma$) is close to that of real photon objects. Exploiting the differences in shape of the track-isolation ($p^{\text{iso}}_{\text{T}}$), defined as the scalar sum of all track momenta within a cone of radius 0.2 with respect to the photon candidate, allows for a discrimination between real photons and hadrons. The final result is extracted by a template-based likelihood fit on $p^{\text{iso}}_{\text{T}}$ from data candidates in the electron and muon channels simultaneously see Fig. 3.

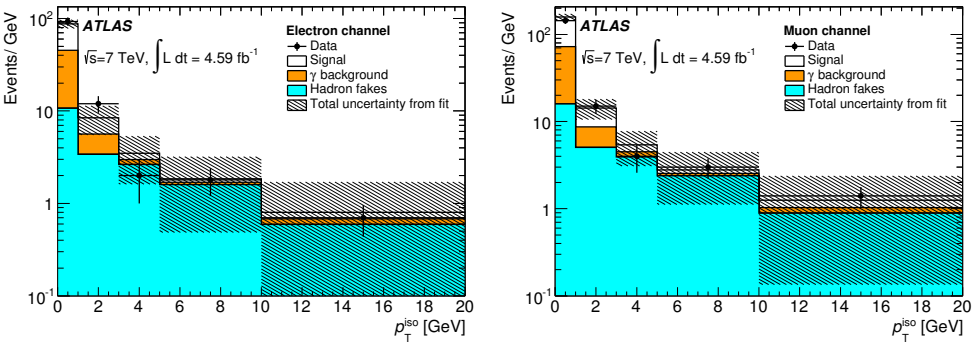

Figure 3. Results of the combined likelihood fit using the track-isolation ($p^{\text{iso}}_{\text{T}}$) distributions as the discriminating variable for the electron channel (left) and the muon channel (right). The contribution from $t\bar{t}\gamma$ events is labeled as "Signal", prompt-photon background is labeled "γ backgrounds", the contribution from hadrons misidentified as photons (as estimated by the template fit) is labeled as "Hadron fakes" [5].

The $\sigma^{\text{fid.}}_{t\bar{t}\gamma}$ is defined in a phase-space within the kinematic and geometrical detector acceptance. The definition of particles belonging to the phase-space is motivated by imposing experimentally observable selection criteria. This definition diminishes the model-dependency and augments the reproducibility of the result. The result measured cross section [5],

$$\sigma^{\text{fid.}}_{t\bar{t}\gamma} = 63 \pm 8\,(\text{stat.})\,{}^{17}_{-13}\,(\text{syst.}) \pm 1\,(\text{lumi.})\,\text{fb}, \tag{5}$$

is in good agreement with that of leading order calculation in the fiducial phase-space normalised to fraction of the next-to-leading order to leading order prediction [6] of 48 ± 10 fb.

3.2 Production cross section of $t\bar{t}$ paris in association with a W or Z–boson

Depending on the decays of the top quarks, W and Z–bosons the number of final state prompt isolated leptons may vary between zero and four. Only channels with two (both with same-sign and opposite-sign charge), three, and four leptons are considered in this measurement. Each channel is divided into multiple regions in data in order to enhance the sensitivity to the $t\bar{t}Z$ and $t\bar{t}W$ cross sections. The production cross sections for $t\bar{t}W$ ($\sigma_{t\bar{t}W}$) and $t\bar{t}Z$ ($\sigma_{t\bar{t}Z}$) are determined simultaneously using a binned maximum-likelihood fit over all regions and discriminant bins considered in the analysis [7]. The fit results are summarised in Fig. 4.

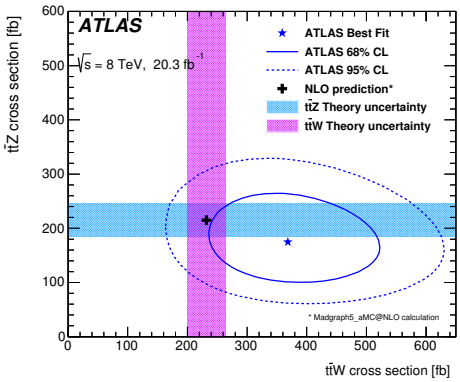

Figure 4. The result of the simultaneous fit to the $t\bar{t}W$ and $t\bar{t}Z$ cross sections along with the 68% and 95% Confidence Level (CL) uncertainty contours. The shaded areas correspond to 14% uncertainty, which includes renormalisation and factorisation scale uncertainties as well as parton density function uncertainties including α_s variations [7].

The results are [7]

$$\sigma_{t\bar{t}W} = 369\ ^{86}_{-79}\ \text{(stat.)}\ \pm 44\ \text{(syst.)}\ \text{fb} \tag{6}$$

for the $t\bar{t}W$ production and

$$\sigma_{t\bar{t}Z} = 176\ ^{52}_{-48}\ \text{(stat.)}\ \pm 24\ \text{(syst.)}\ \text{fb} \tag{7}$$

for the $t\bar{t}Z$ production. It can be seen in Fig. 4 that the results are in good agreement with the theoretical prediction.

4 Charge asymmetry

The difference in rapidity between top and anti-top quarks in proton–proton collisions is referred to as the charge asymmetry (A_C). At hadron colliders and the leading order contribution of A_C is zero, because of the symmetric $t\bar{t}$ production under the exchange of top and anti-top quarks. At next-to-leading order the $t\bar{t}$ paris produced from quark anti-quark annihilation, due to interferences with initial- and final-state gluon emission, produce an asymmetry in rapidity. The SM predicts values of

A_C to be of the percent level with next-to-leading order accuracy [8]. Several extensions of the SM, for example models with anomalous vector or axial-vector couplings (axigluons), predict higher values of A_C. Moreover, these models predict also differences in the spectra of A_C as a function of invariant mass of the $t\bar{t}$ system ($m_{t\bar{t}}$), of the longitudinal boost of $t\bar{t}$ ($\beta_{z,t\bar{t}}$) and of the transverse momentum of the $t\bar{t}$ system ($p_{T,t\bar{t}}$). Therefore, the measurement of A_C both inclusively and differentially is of great interest.

The analysis is carried out in the single lepton plus jets plus missing transverse momentum final state, and the event kinematics are reconstructed using a kinematic likelihood fit [10]. The reconstructed rapidity spectra are corrected for acceptance and detector resolution effects using a *Bayesian* unfolding procedure [9]. The final measured A_C is extracted from a likelihood fit, where the rapidity spectra are further discriminated with respect to the measured lepton charge.

The differential results of A_C are shown in Fig. 5 and they are compatible with the SM prediction. The inclusive $t\bar{t}$ production charge asymmetry is measured to be [9]

$$A_C = 0.009 \pm 0.005 \text{ (stat.} \oplus \text{syst.)}, \tag{8}$$

compatible with the SM prediction, $A_C = 0.0111 \pm 0.0004$ [8].

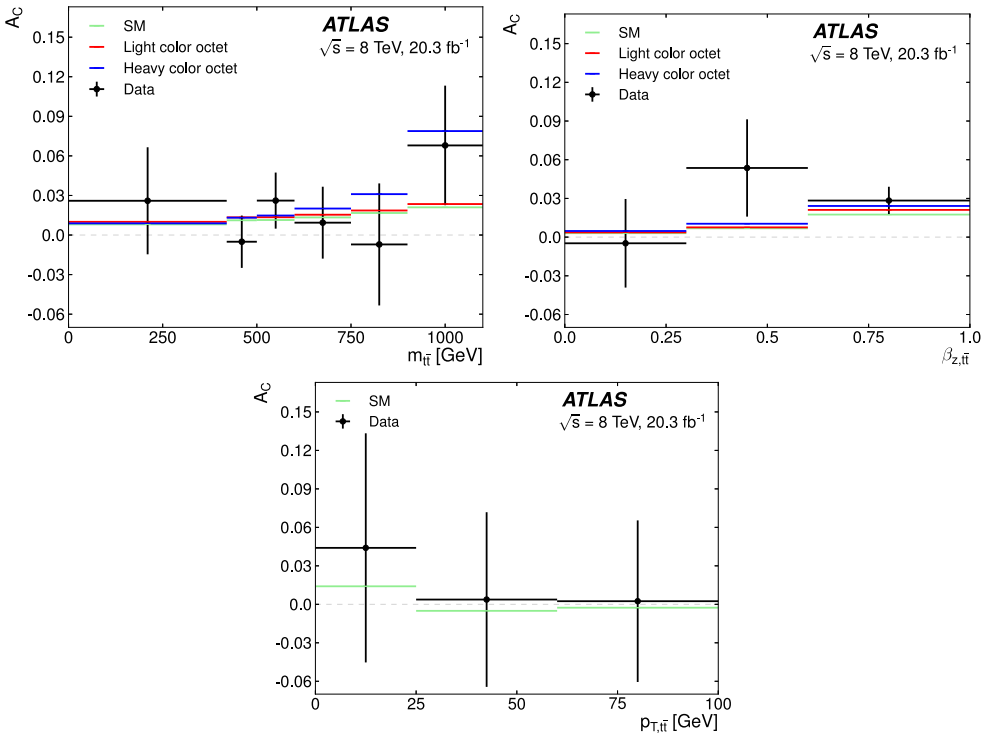

Figure 5. Measured A_C values as a function of bin-averaged $m_{t\bar{t}}$ (top left), $\beta_{z,t\bar{t}}$ (top right) and $p_{T,t\bar{t}}$ (bottom) compared with predictions for the SM [8] and for right-handed colour octets [11] with masses below the $t\bar{t}$ threshold and beyond the kinematic reach of current LHC searches. The beyond the standard model predictions are shown only for the two top plots. [9].

5 Conclusions

These proceeding reviewed some of the most recent results on the top quark measurements performed by the ATLAS detector. These results are based upon datasets of 4.59 fb^{-1} and of 20.3 fb^{-1} of proton–proton collisions delivered by the LHC at the centres-of-mass energy of $\sqrt{s}$ = 7 TeV and of $\sqrt{s}$ = 8 TeV, respectively. In particular, the measurements of the top quark mass, the cross section of $t\bar{t}$ production in association of vector bosons (W, Z and γ) and the measurement of the charge asymmetry were detailed.

The abundant production of $t\bar{t}$ pairs at the LHC allows for evermore precise measurements of the top quark properties leading to stringent tests of the SM and to searches for new phenomena trough deviations from the expected SM predictions.

References

[1] ATLAS Collaboration, *JHEP* **10** (2015), doi:10.1007/JHEP10(2015)121.
[2] ATLAS Collaboration, *EPJ* **C75** (2015), 7, doi:10.1140/epjc/s10052-015-3544-0.
[3] S. Alioli *et al.*, *EPJ* **C73** (2013), 2438, arXiv:1303.6415.
[4] B. Lillie J. Shu and T. M. P. Tait, *JHEP* **04**, (2008), 87.
[5] ATLAS Collaboration, *PRD* **91** (2015), 072007.
[6] K. Melnikov, A. Scharf, and M. Schulze, *PRD* **83** (2011), 074013.
[7] ATLAS Collaboration, (2015), arXiv:1509.05276.
[8] W. Bernreuther and Z.-G. Si, *PRD* **86** (2012), 034026, doi:10.1103/PhysRevD.86.034026.
[9] ATLAS Collaboration, (2015), arXiv:1509.02358.
[10] J. Erdmann *et al.*, *NIM* **A748** (2014), 18-25, doi:10.1016/j.nima.2014.02.029.
[11] J. A. Aguilar-Saavedra, *JHEP* **08** (2014), 172, doi:10.1007/JHEP08(2014)172.